Supplementary material

The Role of Terminal and Bridge Ligands on the Molecular Upconversion of Lanthanide(III) 1D Coordination Polymers

Stefano A. de Andrade,[a] Airton G. Bispo-Jr,[a,b] Deborah de A. Simoni,[a] Javier A. Ellena,[c] Italo O. Mazali,[b] and Fernando A. Sigoli[a]*

[a] Institute of Chemistry, State University of Campinas, Campinas, São Paulo 13083-970, Brazil.

[b] Institute of Chemistry, University of São Paulo, São Paulo, São Paulo 05508-000, Brazil.

[c] Institute of Physics, University of São Paulo, São Carlos, São Paulo 13566-590, Brazil.

Index

Supplementary Note S1 – Synthesis of the precursors and characterization

Chemicals

Erbium oxide (Er_2O_3, 99.9%, Aldrich), ytterbium oxide (Yb_2O_3, 99.9%, Aldrich), 2,4-pentanedione (acetyl acetone or acac, ≥99,9%, Aldritch), 1,1,1-trifluoro-2,4-pentanedione (trifluoroacetylacetone or tfa, 98%, Aldritch), 1,1,1,5,5,5-hexafluoro-2,4-pentanedione (hexafluoroacetylacetone or hfa, 98%, Aldritch), 1,2-Bis(diphenylphosphino)-ethane (dppe, 98%, Aldritch), 1,4-Bis(diphenylphosphino)-butane (dppb, 98%, Aldritch), ethanol (EtOH, 99%, Synth), sodium hydroxide (97%, Química Moderna), hydrochloric acid (HCl, 36.5%, Merck), hydrogen peroxide (H_2O_2, 29%, Synth), and Toluene ($C_6H_5CH_3$, 99,5%, Synth) were used without any further purification.

Synthesis of $[Ln(acac)_3(H_2O)_2]$, $[Ln(tfa)_3(H_2O)_2]$, and $[Ln(hfa)_3(H_2O)_2]$ precursor complexes.

The lanthanide precursor complexes $[Ln(acac)_3(H_2O)_2]$, $[Ln(tfa)_3(H_2O)_2]$ and $[Ln(hfa)_3(H_2O)_2]$, Ln = Er, Yb, acac = 2,4-pentanedione, tfa = 1,1,1-trifluoro-2,4-pentanedione, hfa = 1,1,1,5,5,5-hexafluoro-2,4-pentanedione, were synthesized following a well stablished pathway in literature (Figure S1)[1]. For that, 3.6 mmols of the ligand (acac, tfa or hfa) were weighted, put in a Becker with 5 mL of distilled water, and quickly 3.6 mmols of NaOH were added dropwise. In another Becker, 0.6 mmols of $YbCl_3$ and 0.6 mmols of $ErCl_3$ in aqueous solution were mixed and added dropwise to the ligand solution. The precursor complexes precipitated quickly, and the synthesis was left for a couple more hours, with the observation of a larger amount of precipitate the next morning, The precipitate was filtered and dried in vacuum. Yields: $[Ln(acac)_3(H_2O)_2]$ = 65%-72%, $[Ln(tfa)_3(H_2O)_2]$ = 48%-52%, $[Ln(hfa)_3(H_2O)_2]$ = 22%-27%.

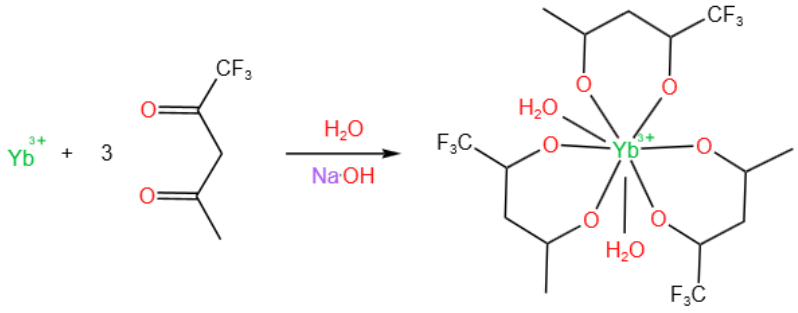

Figure S1. Synthetic pathway for the synthesis of the Ln^{III} complex precursors, using the $[Yb(tfa)_3(H_2O)_2]$ case as example. The same process goes for acac and hfa ligands in place of tfa, and Er^{III} in place of Yb^{III}.

Synthesis of Phospine Oxides Bridging Ligands L

The phosphine oxides bridge ligands L = [(diphenylphosphoryl)R](diphenyl)phosphine oxide (R = ethyl or butyl), named dppeo or dppbo, respectively, were synthesized from bis(diphenylphosphino)R, called dppe and dppb (for R = ethyl or butyl, respectively). The pathway followed a well-spread literature protocol (Figure S2)[2]. For that, H_2O_2 was added dropwise in a round bottom flask containing 30 mL toluene solution and dissolved dppe or dppb, under stirring over the course of 30 minutes at 0°C. The reaction was left over three hours with the intent of optimizing the yield, and more H_2O_2 was added over the course of time. The precipitate was filtered 5 times with toluene and left to dry. Yield: > 90%.

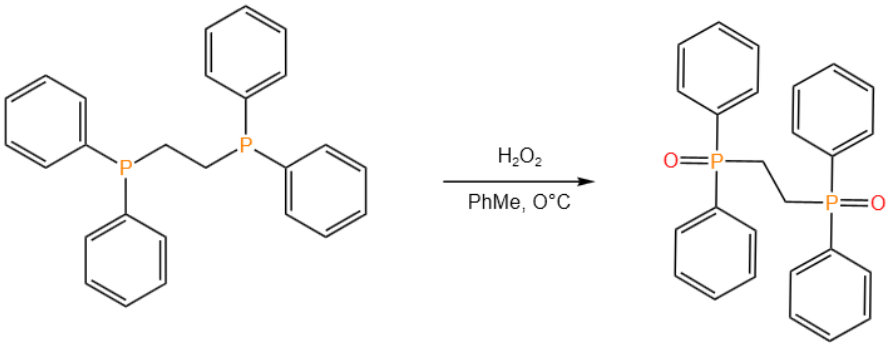

Figure S2. Synthetic pathway for the dppeo ligand. The same process was followed for dppbo.

Characterization apparatus

The single-crystal X-Ray diffraction (SC-XRD) data collection of **1** and **4** were performed employing the Rigaku XtaLAB Synergy-S diffractometer, equipped with the HyPix-6000HE detector and MoK_α radiation (λ = 0.71073 Å at 120 K) microfocus with a sealed X-ray source. The SC-XRD data of **2**, **3** and **5** were collected in a BRUKER APEX II Duo CCD DETECTOR DIFFRACTOMETER equipped with a fine-focus sealed tube, Mo Kα (λ = 0.71073 Å at 120 K), as radiation source. The crystals were selected and mounted in cryoloop with mineral oil. The collection strategies and cell refinement for **1** and **4** were carried out using the CrysAlisPro. Moreover, the structures **1** and **4** were solved by direct methods employing SHELXLT XT (version 2014/4) and refined using SHELX 64.[3] For **2**, **3**, and **5**, the collection strategies and cell refinement were carried out using the APEX2 (Bruker, 2010) and the structures were solved using the SHELXS97 (Sheldrick, 2008) software.[4] A multi-scan absorption correction was performed for all the compositions. The CIF file of **1** - **5** were deposited in the Cambridge Structural Database with CCDC numbers of 2381906, 2381909, 2381910, 2381911, and 2381913, respectively. Copies of the data can be accessed, free of charge, via www.ccdc.ac.uk.

Powder X-ray diffraction within 10–60° was measured using a Shimadzu XRD 7000 (Cu Kα, λ = 1.5418 Å) diffractometer operating at 40 kV and 30 mA, with scan rate of 0.5° min^{-1}

FTIR spectra and data obtention of solid-state materials were carried out on a Agilent Cary 600 Series FTIR Spectrophotometer (660) in the range of 4,000 to 400 cm^{-1} with a resolution of 1 cm^{-1} with the help of an attenuated total reflectance (ATR) accessory.

Upconversion emission spectra were collected in a Fluorog-3 (Horiba FL3-22-iHR320) equipped with a double excitation (1200 groves nm^{-1}, blazed 330 nm), and a double emission (1200 groves nm^{-1}, blazed 500 nm) monochromator. The emission spectra were obtained using a 980 nm laser (Crystalaser DL980-1W-T0) with variable power densities as an excitation source. The emission spectra were corrected according to the photodetector spectral response.

Supplementary Note S2 – Crystallographic data

Table S1. Crystal data and some refinement parameters for **1** - **5**.

	1	2	3	4	5
Empirical formula	$C_{41}H_{36}ErF_9O_8P_2Yb$	$C_{41}H_{27}F_{18}O_8P_2Tb$	$C_{43}H_{40}F_9O_8P_2Tb$	$C_{43}H_{31}F_{18}O_8P_2Yb$	$C_{56}H_{70}O_{16}P_2Yb_2$
CCDC	2381906	2381909	2381910	2381911	2381913
Formula Weight / g mol^{-1}	1056.90	1210.50	1076.62	1252.66	1407.14
Temperature / K	120	120	120	120	120
Wavelength / Å	0.71073	0.71073	0.71073	0.71073	0.71073
Crystal system	Triclinic	Triclinic	Triclinic	Triclinic	Triclinic
Space group	$P\bar{1}$	$P\bar{1}$	$P\bar{1}$	$P\bar{1}$	$P\bar{1}$
Unit cell dimensions a, b, c / Å α, β, γ/ °	a=12.6940(8) b=12.9971(8) c=14.2063(8) α =105.364(1) β =102.025(1) γ =103.618(1)	a=13.0460(13) b=13.2860(14) c=14.0894(15) α =105.947(2) β =102.243(2) γ=102.910(2)	a=11.4899(11) b=13.4321(12) c=15.2194(14) α =82.156(2) β=72.742(2) γ =88.205(2)	a=13.1953(10) b=13.2045(10) c=15.0669(10) α=91.991(2) β=102.513(2) γ=108.947(2)	a=10.8843(10) b=12.0573(10) c=12.1748(10) α=116.489(2) β =94.107(2) γ =91.258(2)
Volume / Å^3	2102.9(2)	2189.2(4)	2222.0(4)	2408.2(3)	1423.8(2)
Z	2	2	2	2	1
Density (calculated) / g cm^{-3}	1.669	1.836	1.609	1.727	1.641
F(000)	1050.0	1188.0	1076.0	1230.0	704.0
R (reflections)	0.0282 (7806)	0.0318 (8013)	0.0205 (10626)	0.0351 (7604)	0.0129 (7549)
wR^2 (reflections)	0.0538 (9241)	0.0618 (9558)	0.0480 (11486)	0.0772 (9030)	0.0344 (7726)
Data completeness	0.994	0.997	1.000	0.988	1.000

Table S2. Shape analysis of the synthesized polymers and dimer utilizing SHAPE 2.1[5]. The value presented are the continuous shape measures (CShM, dimensionless) for each idealized geometry.

Idealized Geometry	Short name	Point group	1	2	3	4	5
Square Antiprism	SAPR-8	*D4d*	**0.183**	**0.388**	1.421	**0.331**	**0.389**
Triangular dodecahedron	TDD-8	*D2d*	2.224	1.774	**0.482**	1.736	1.792
Biaugmented trigonal prism	BTPR-8	*C2v*	1.855	1.500	1.577	1.617	1.823
Biaugmented trigonal prism J50	JBTPR-8	*C2v*	2.328	1.876	1.945	1.977	2.359
Snub diphenoid J84	JSD-8	*D2d*	4.452	3.620	2.693	3.824	4.742
Cube	CU-8	*Oh*	10.142	10.425	9.490	10.331	9.122
Triakis tetrahedron	TT-8	*Td*	10.982	11.237	10.192	10.946	9.986
Hexagonal bipyramid	HBPY-8	*D6h*	16.589	16.237	16.246	17.193	15.296
Johnson gyrobifastigium J26	JGBF-8	*D2d*	15.254	14.234	13.717	15.416	14.735
Heptagonal pyramid	HPY-8	*C7v*	23.546	24.038	23.822	23.470	23.526
Elongated trigonal bipyramid	ETBPY-8	*D3h*	24.057	24.329	24.859	24.328	23.925
Johnson elongated triangular bipyramid J14	JETBPY-8	*D3h*	28.433	28.620	29.386	28.033	28.704

Table S3. Selected Ln-O bond distances in the coordination spheres. O1-O6 are β-biketone oxygen. O7-O8 are phosphine oxide oxigens for the coordination polymers.

	1	2	3	4	5
Bond	Distance (Å)	Distance (Å)	Distance (Å)	Distance (Å)	Distance (Å)
Ln^{III} – O1	2.3358(19)	2.248(2)	2.2875(13)	2.339(3)	2.3249(10)
Ln^{III} – O2	2.2731(19)	2.242(2)	2.2417(13)	2.240(3)	2.3794(10)
Ln^{III} – O3	2.3502(19)	2.364(2)	2.3632(13)	2.334(3)	2.3160(11)
Ln^{III} – O4	2.3315(19)	2.364(2)	2.3396(13)	2.361(3)	2.3134(11)
Ln^{III} – O5	2.3444(19)	2.351(2)	2.3574(13)	2.308(3)	2.2945(11)
Ln^{III} – O6	2.2622(18)	2.330(2)	2.2961(13)	2.218(3)	2.333(1)
Ln^{III} – O7	2.2731(19)	2.307(2)	2.3251(14)	2.388(3)	2.3629(10)
Ln^{III} – O8	2.3309(19)	2.373(2)	2.3166(14)	2.355(3)	2.2778(11)
β-diketone average	2.3162	2.3165	2.3142	2.300	2.32564

Table S4. Bond angles for the coordination spheres in all the synthesized compounds.

	1	2	3	4	5
Bond	Angle (°)	Angle (°)	Angle (°)	Angle (°)	Angle (°)
O3-Ln-O4	72.38(7)	73.41(7)	73.50(5)	72.49(9)	72.93(4)
O5-Ln-O6	74.96(7)	71.91(7)	74.51(5)	71.21(11)	73.44(4)
O7-Ln-O8	72.29(7)	72.21(7)	72.26(5)	74.3(1)	73.56(4)
P1-O1-Ln	154.32(13)	161.07(8)	161.07(8)	153.16(17)	156.21(7)
P2-O2-Ln	158.64(12)	177.14(9)	177.14(9)	158.38(17)	----------

Table S5. Chain linearity angle and shortest distances between lanthanide cores for the synthesized compounds.

	1	2	3	4	5
Ln-Ln-Ln Angle / °	173.225(4)	174.984(5)	75.921(3)	178.187(4)	----------
Ln-Ln intramolecular Distance / Å	8.2958(4)	8.4443(7)	10.7704(8)	9.2853(6)	8.8327(7)
Ln --- Ln intermolecular distance / Å	11.6276(6)	12.4334(9)	8.1045(7)	11.7562(7)	5.8324(5)

Supplementary Note S3 – Inter/intramolecular interactions

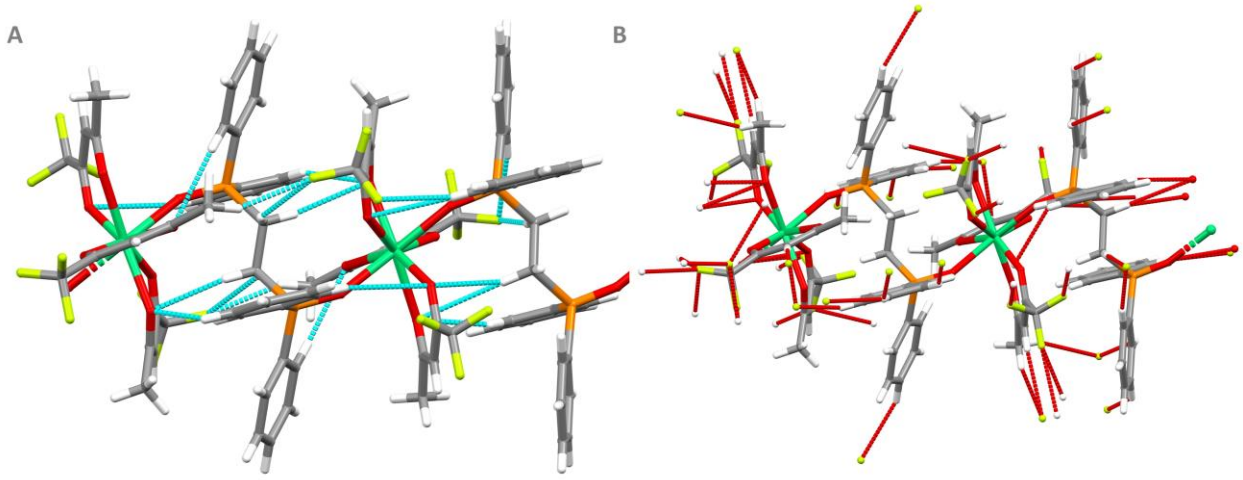

Figure S3. (a) Intra and (b) intermolecular hydrogen bonds of **1**.

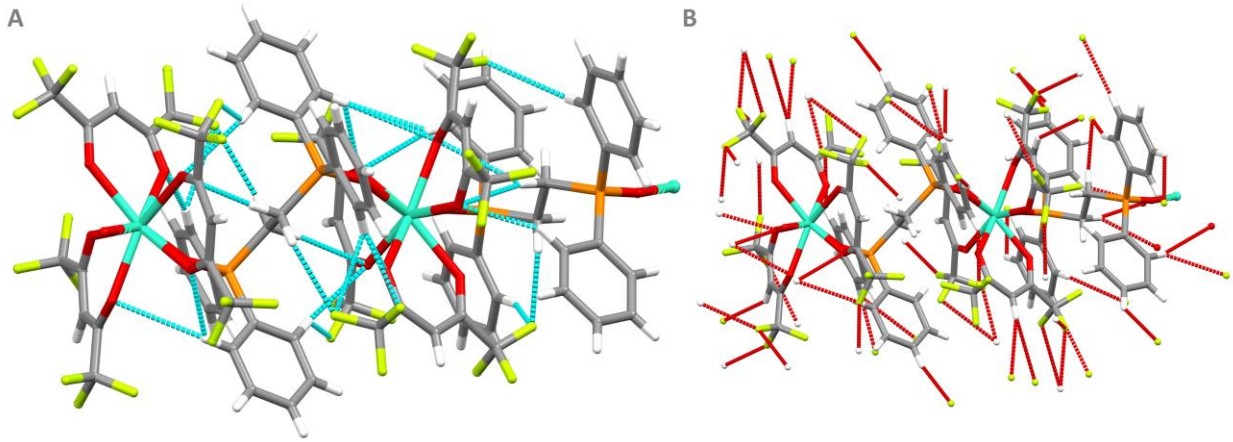

Figure S4. (a) Intra and (b) intermolecular hydrogen bonds of **2**.

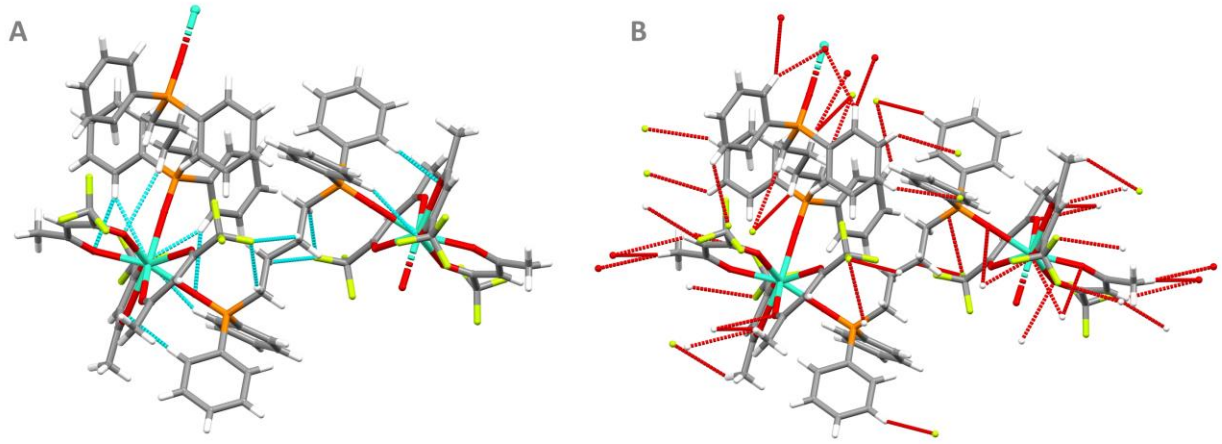

Figure S5. (a) Intra and (b) intermolecular hydrogen bonds of **3**.

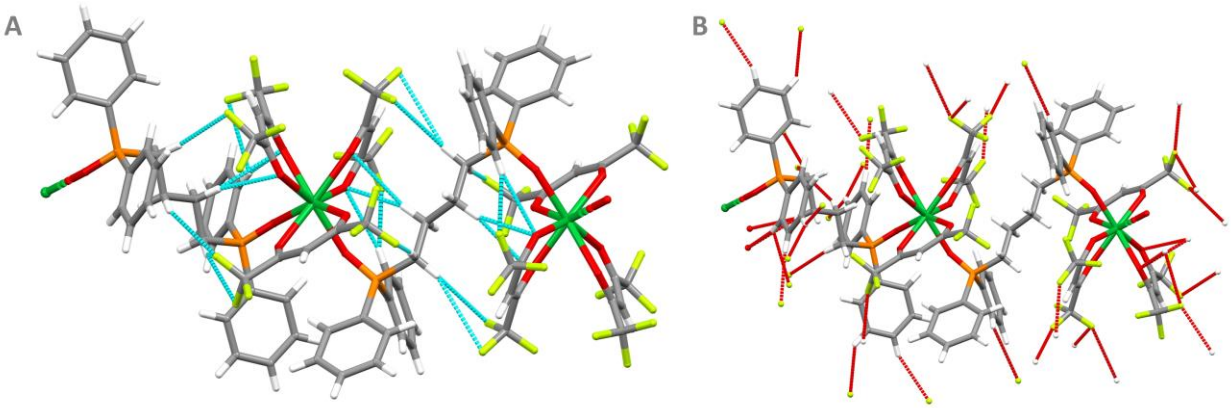

Figure S6. (a) Intra and (b) intermolecular hydrogen bonds of **4**.

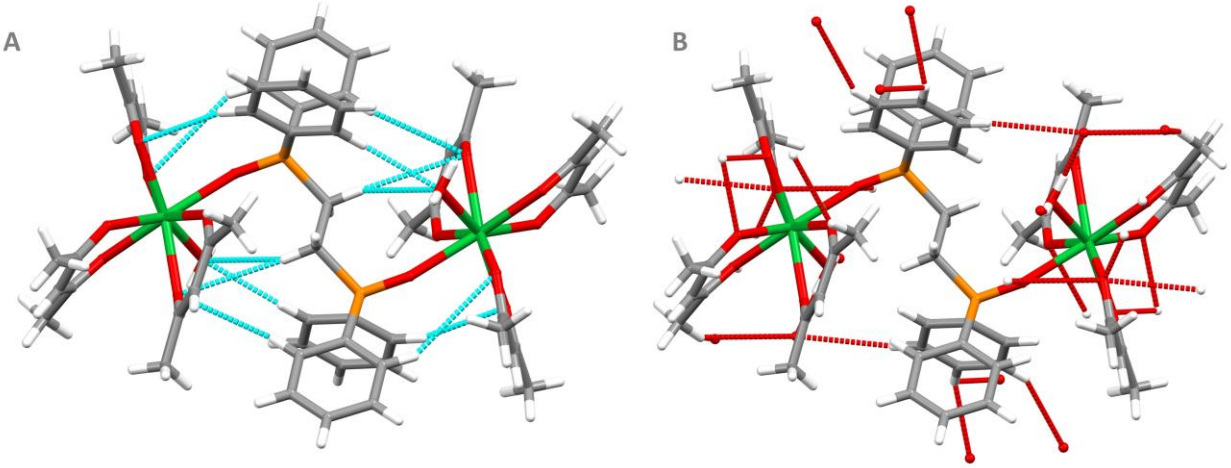

Figure S7. (a) Intra and (b) intermolecular hydrogen bonds of **5**.

Table S6. Intra/intermolecular H-bond distances for **1**.

Intramolecular H-bonds		
Atom 1	**Atom 2**	**Distance / Å**
F1B	H226	2.566
F1B	H23A	2.619
F1C	H215	2.727
F2C	H13A	3.243
F2C	H5BC	2.49
O1A	H111	3.093
O1A	H23B	2.714
O1C	H215	2.946
O2A	H211	2.519
O2A	H23B	3.044
O2B	H125	2.685
O2C	H115	2.479
O2C	H13B	2.638
Intermolecular H-Bonds		
H211	O2A	2.519
H23B	O1A	2.714
H23B	O2A	3.044
H215	F1C	2.727
H215	O1C	2.946
H226	F1B	2.566
H23A	F1B	2.619
F1A	H113	2.835
F2A	H112	2.951
H113	F1B	3.255
H114	F3B	2.792
F2B	H3B	2.876
F3B	H3B	2.738
F3A	H3A	2.881
F3A	H5AA	2.608
F1C	H223	3.004
F3C	H5AB	3.071
F3C	H222	2.674
H123	F3B	2.87

Table S7. Intra/intermolecular H-bond distances for **2**.

Intramolecular H-bonds		
Atom 1	**Atom 2**	**Distance / Å**
F1	H19	2.718
F1	H26A	2.617
F2	H19	2.533
F4	H2	2.631
F4	H13A	2.494
F9	H2	2.801
F15	H25	2.455
F18	H12	2.872
O3	H19	2.726
O5	H21	3.005
O5	H13B	2.819
O6	H8	2.554
O6	H13B	3.005
O7	H25	2.64
O7	H26B	2.693
O8	H12	2.951
O8	H21	2.679
Intermolecular H-bonds		
O3	H19	2.726
O5	H21	3.005
O5	H13B	2.819
O6	H8	2.554
O6	H13B	3.005
O7	H25	2.64
O7	H26B	2.693
O8	H12	2.951
O8	H21	2.679
H8	O6	2.554
H13B	O5	2.819
H13B	O6	3.005
H12	O8	2.951

Table S8. Intra/intermolecular H-bond distances for **3**.

Intramolecular H-bonds		
Atom 1	**Atom 2**	**Distance / Å**
H1A	F4	2.665
H2A	F4	2.801
H8	O4	2.522
H14	O3	2.846
H16B	O7	2.901
H18	O1	3.188
H18	O3	2.438
H24	O3	2.854
Intermolecular H-bonds		
H5	F5	2.985
F5	H21	2.881
H25	F3	2.894
H26	F1	2.919
H33A	F9	2.874
H41	O4	3.213
H43C	O4	2.741
H43C	O6	2.749
O1	H18	3.188
H16B	O7	2.901
H18	O3	2.438
H24	O3	2.854
H24	O8	2.768
H16B	F7B	3.198
H15B	F7B	2.869

Table S9. Intra/intermolecular H-bond distances for **4**.

Intramolecular H-bonds		
Atom 1	**Atom 2**	**Distance / Å**
F2C	H13A	2.656
F3B	H23A	3.077
F4A	H13B	3.169
F4B	H225	2.999
F5C	H23B	2.891
F6A	H13B	3.255
F6C	H23B	3.043
F6C	H23D	2.907
H121	F1A	2.64
O1A	H121	2.784
O1A	H13D	2.742
O1B	H23C	2.981
O2A	H13D	2.922
O2B	H225	2.766
O2B	H23C	2.861
Intermolecular H-bonds		
H214	F5C	2.662
H125	F5A	3.013
H213	F4B	2.725
H23A	F3B	3.077
H23D	F6C	2.907
H225	F4B	2.999
H23B	F5C	2.891
H23B	F6C	3.043
H223	F6A	2.865
H224	F3A	2.595
H223	F5A	3.236
H225	O2B	2.766
H23C	O1B	2.981
H23C	O2B	2.861

Table S10. Intra/intermolecular H-bond distances for **5**.

Intramolecular H-bonds		
Atom 1	**Atom 2**	**Distance / Å**
O3	H12	2.516
O3	H29B	3.024
O5	H6	3.025
O5	H29B	3.165
O8	H2	3.283
O9	H8	2.735
O3	H12	2.516
O3	H29B	3.024
Intermolecular H-bonds		
H11	O8	2.906
O1	H22B	3.009
H3A	O7	2.004
H3B	O8	2.096
O8	H22B	3.151
O4	H9	3.06
O6	H10	2.676
O9	H10	2.735

Table S11. F · · · F interaction distances for **1** – **5**.

Intramolecular F · · · F interactions for 2		
Atom 1	**Atom 2**	**Distance / Å**
F1A	F1B	2.752
Intermolecular F · · · F interactions for 2		
F2	F10	2.89
F14	F15	2.907
F15	F15	2.842
Intramolecular F · · · F interactions for 2		
F4	F9	2.792
Intermolecular F · · · F interactions for 4		
F5B	F2B	2.882
F1B	F1B	2.923

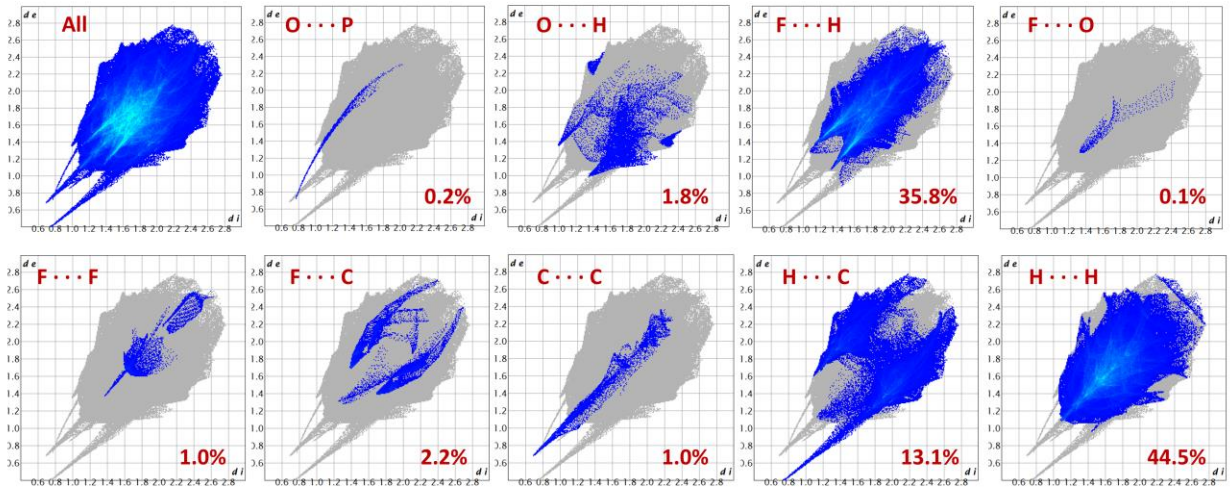

Figure S8. The 2D fingerprint plots of interatomic interactions of **1**, showing the percentages of contacts contributed to the total Hirshfeld surface area of the molecules.

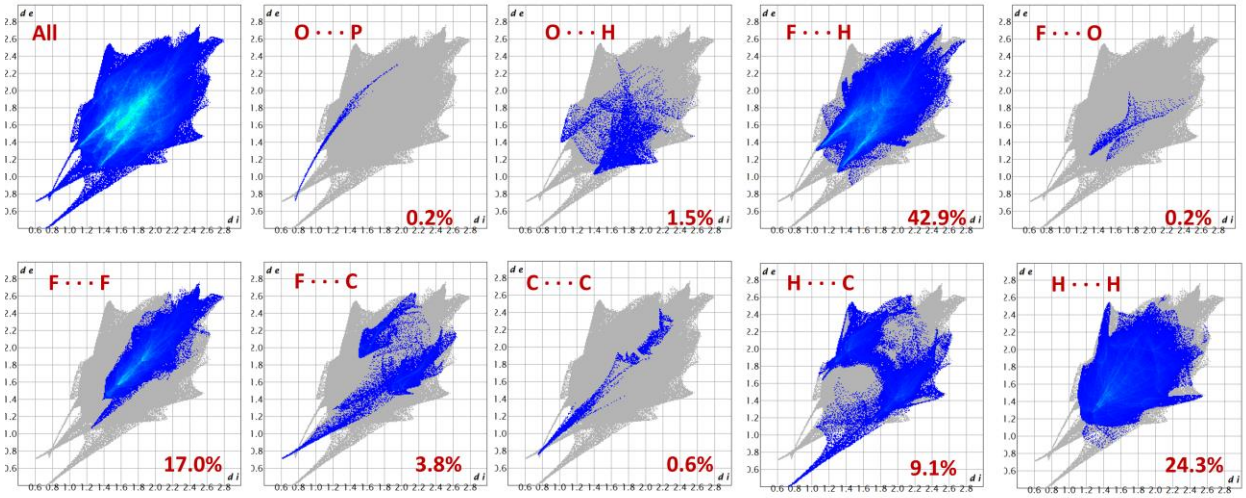

Figure S9. The 2D fingerprint plots of interatomic interactions of **2**, showing the percentages of contacts contributed to the total Hirshfeld surface area of the molecules.

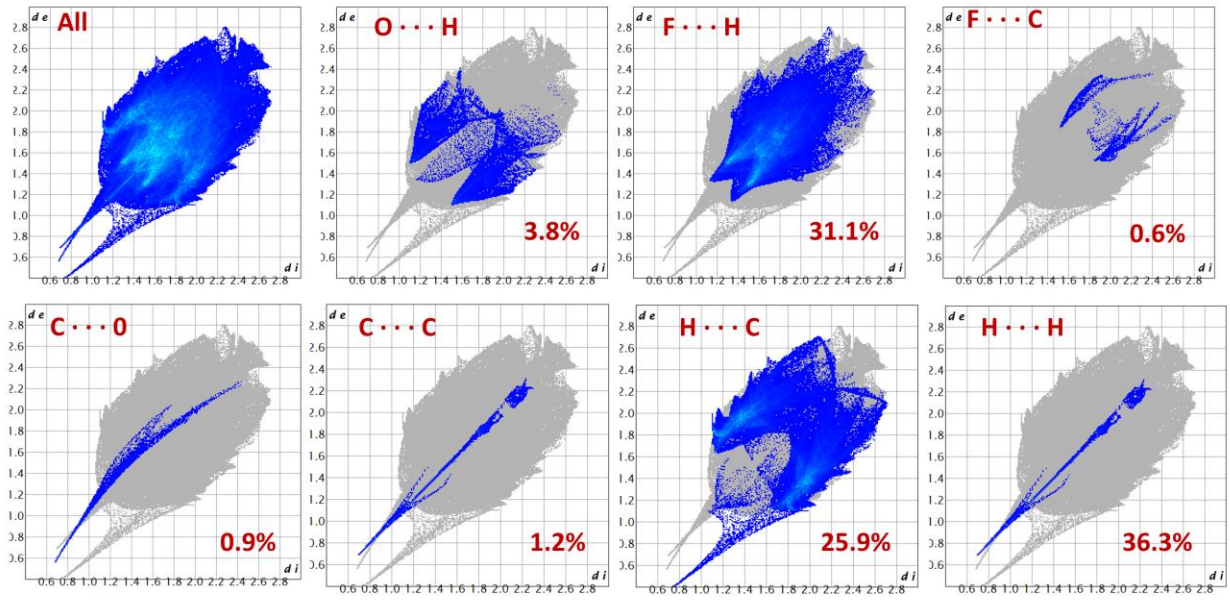

Figure S10. The 2D fingerprint plots of interatomic interactions of **3**, showing the percentages of contacts contributed to the total Hirshfeld surface area of the molecules.

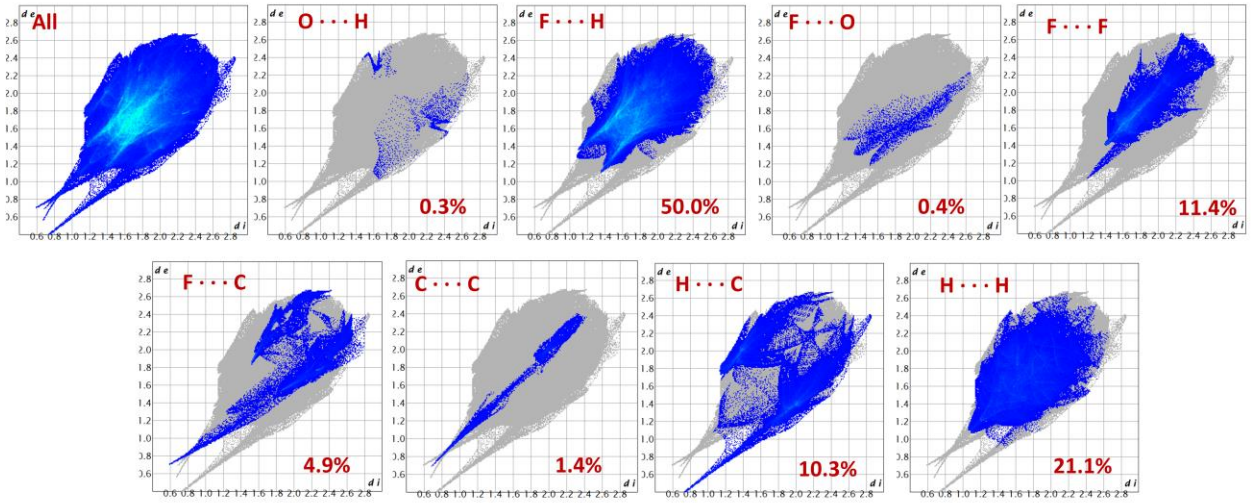

Figure S11. The 2D fingerprint plots of interatomic interactions of **4**, showing the percentages of contacts contributed to the total Hirshfeld surface area of the molecules.

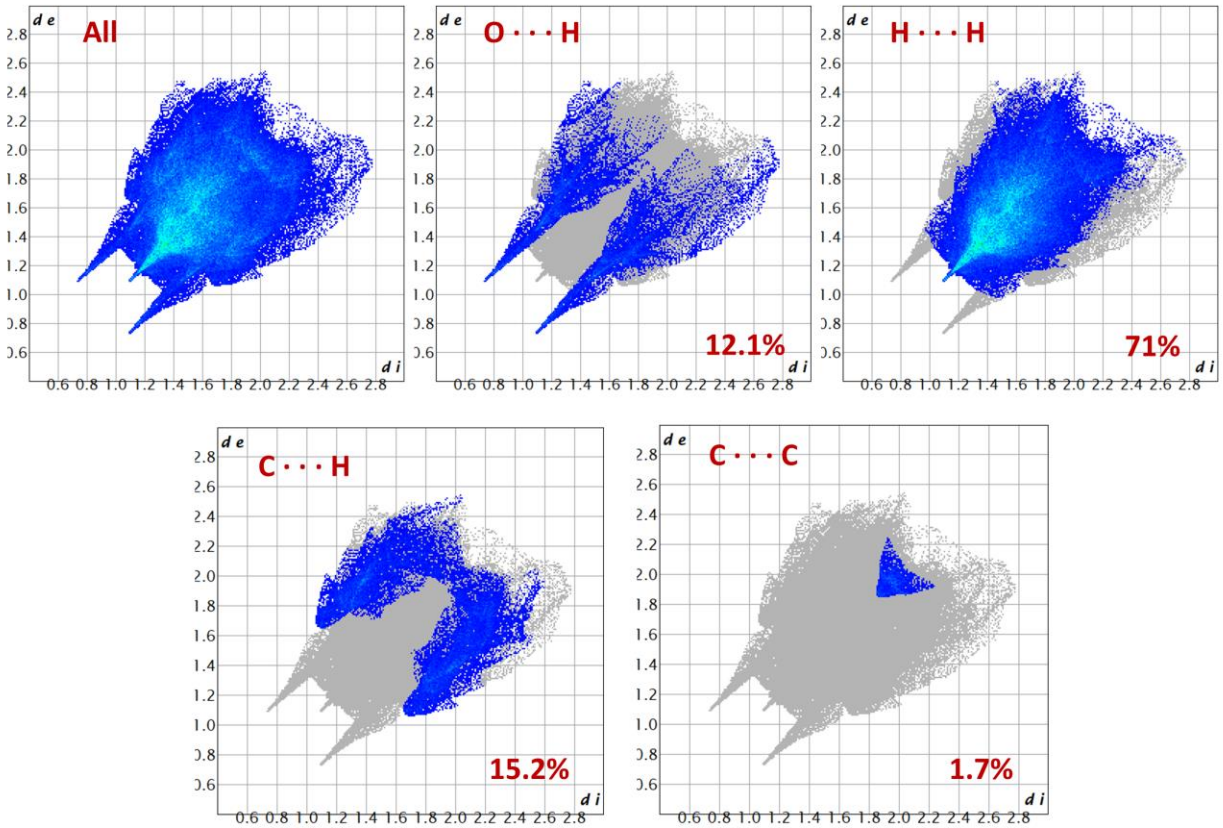

Figure S12. The 2D fingerprint plots of interatomic interactions of **5**, showing the percentages of contacts contributed to the total Hirshfeld surface area of the molecules.

Supplementary Note S4 – Powder X-ray diffraction analyses

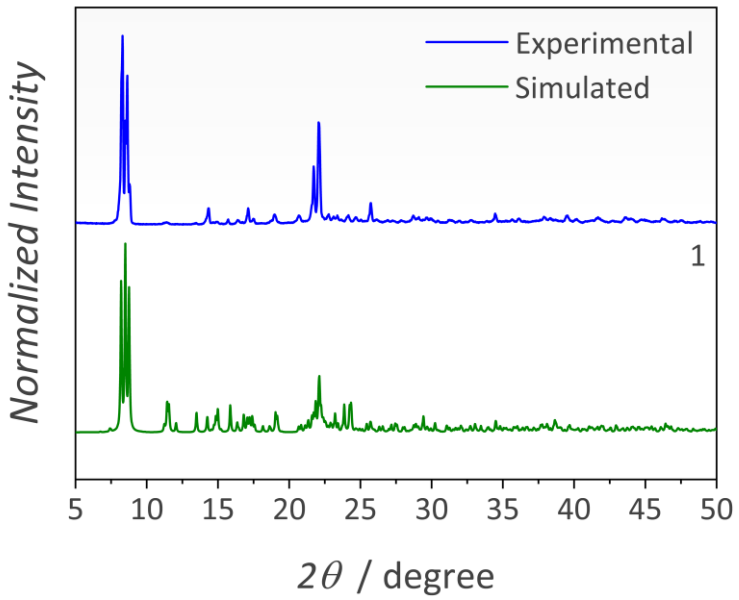

Figure S13. Powder XRD (PXRD) of crashed crystals of **1** compared to the simulated PXRD patter determined from the SC-XRD of the compound.

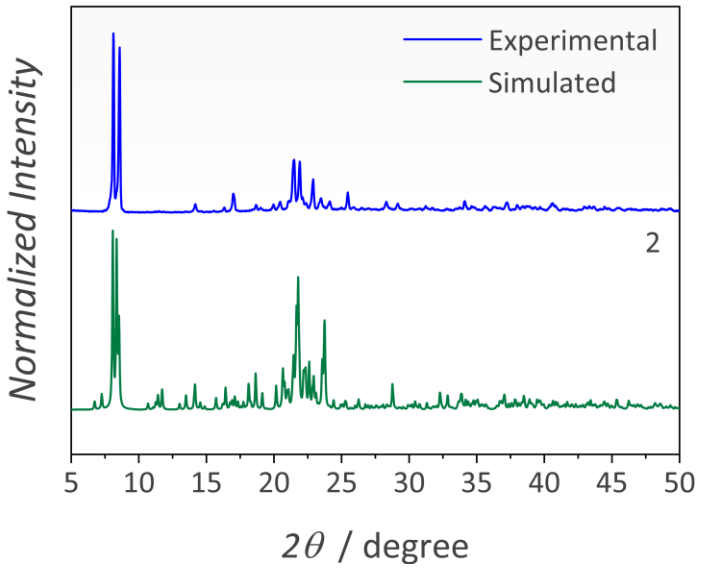

Figure S14. Powder XRD (PXRD) of crashed crystals of **2** compared to the simulated PXRD patter determined from the SC-XRD of the compound.

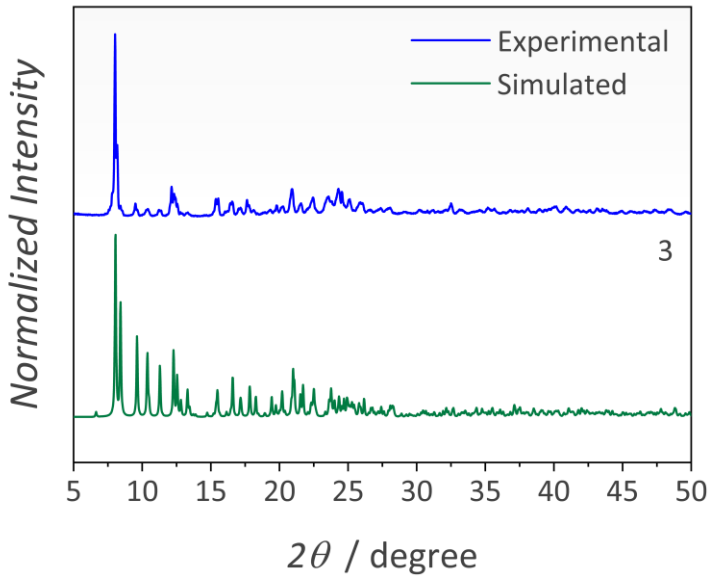

Figure S15. Powder XRD (PXRD) of crashed crystals of **3** compared to the simulated PXRD patter determined from the SC-XRD of the compound.

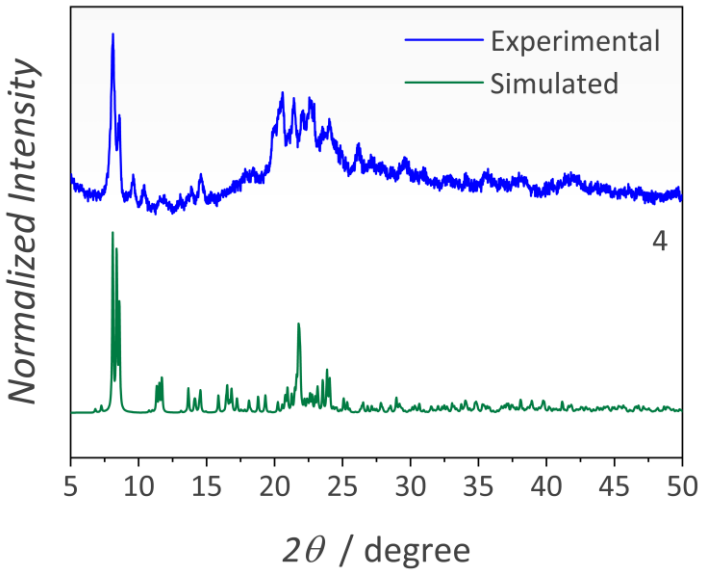

Figure S16. Powder XRD (PXRD) of crashed crystals of **4** compared to the simulated PXRD patter determined from the SC-XRD of the compound.

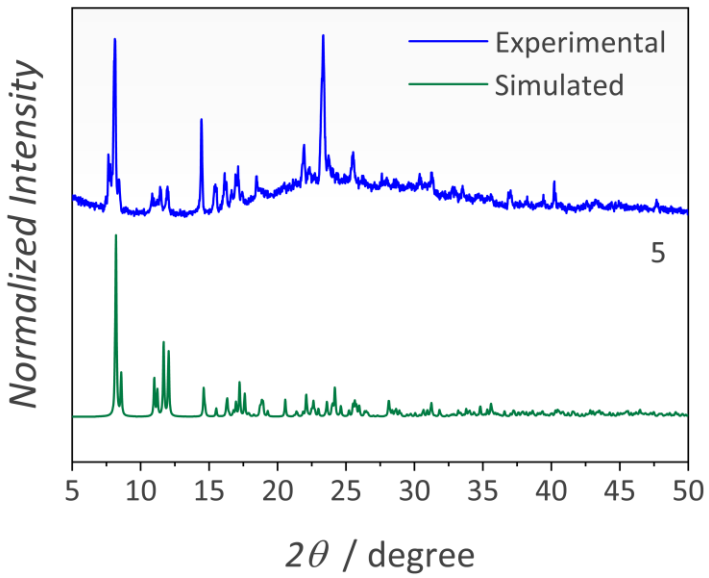

Figure S17. Powder XRD (PXRD) of crashed crystals of **5** compared to the simulated PXRD patter determined from the SC-XRD of the compound.

Supplementary Note S5 – FTIR

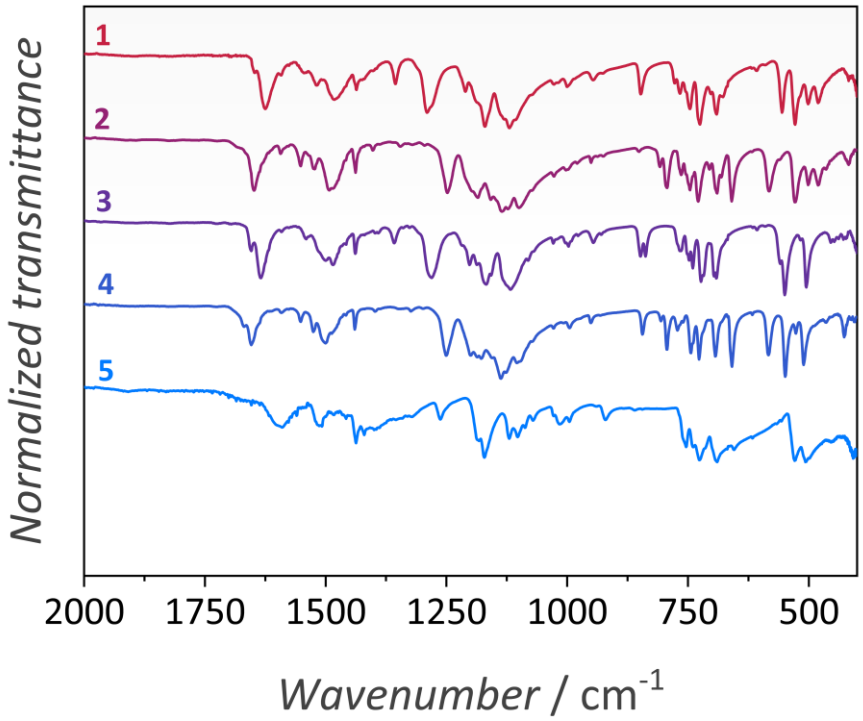

Figure S18. FTIR spectra of **1** - **5**.

Table S12. Position of the C=O and P=O vibrational modes in the FTIR spectra of **1** – **5**.

	1	2	3	4	5
C=O	1625 cm^{-1}	1632 cm^{-1}	1648 cm^{-1}	1653 cm^{-1}	1593 cm^{-1}
P=O	1121 cm^{-1}	1117 cm^{-1}	1099 cm^{-1}	1102 cm^{-1}	1120 cm^{-1}

Supplementary Note S6 – Additional photoluminescence data

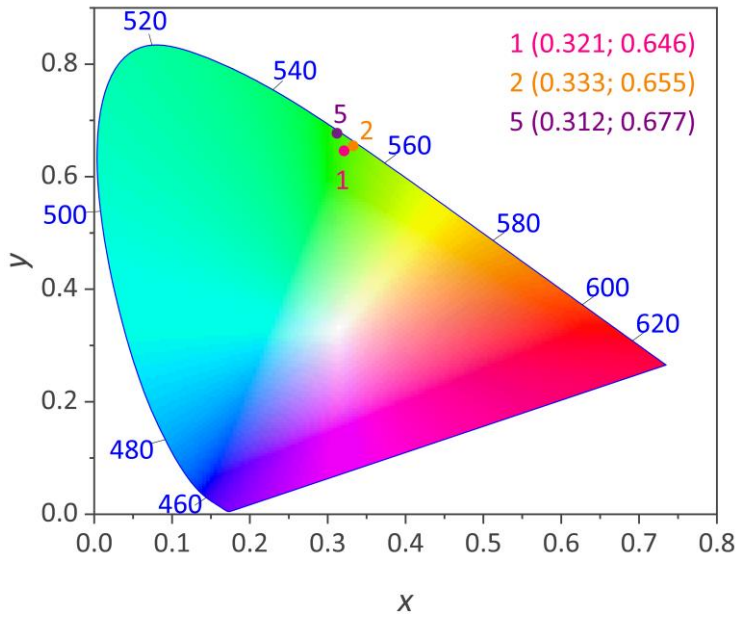

Figure S19. 1931 *Commission Internationale de L'éclairage* (CIE) colour coordinate diagram calculated from the emission spectrum of **1**, **2**, and **5**.

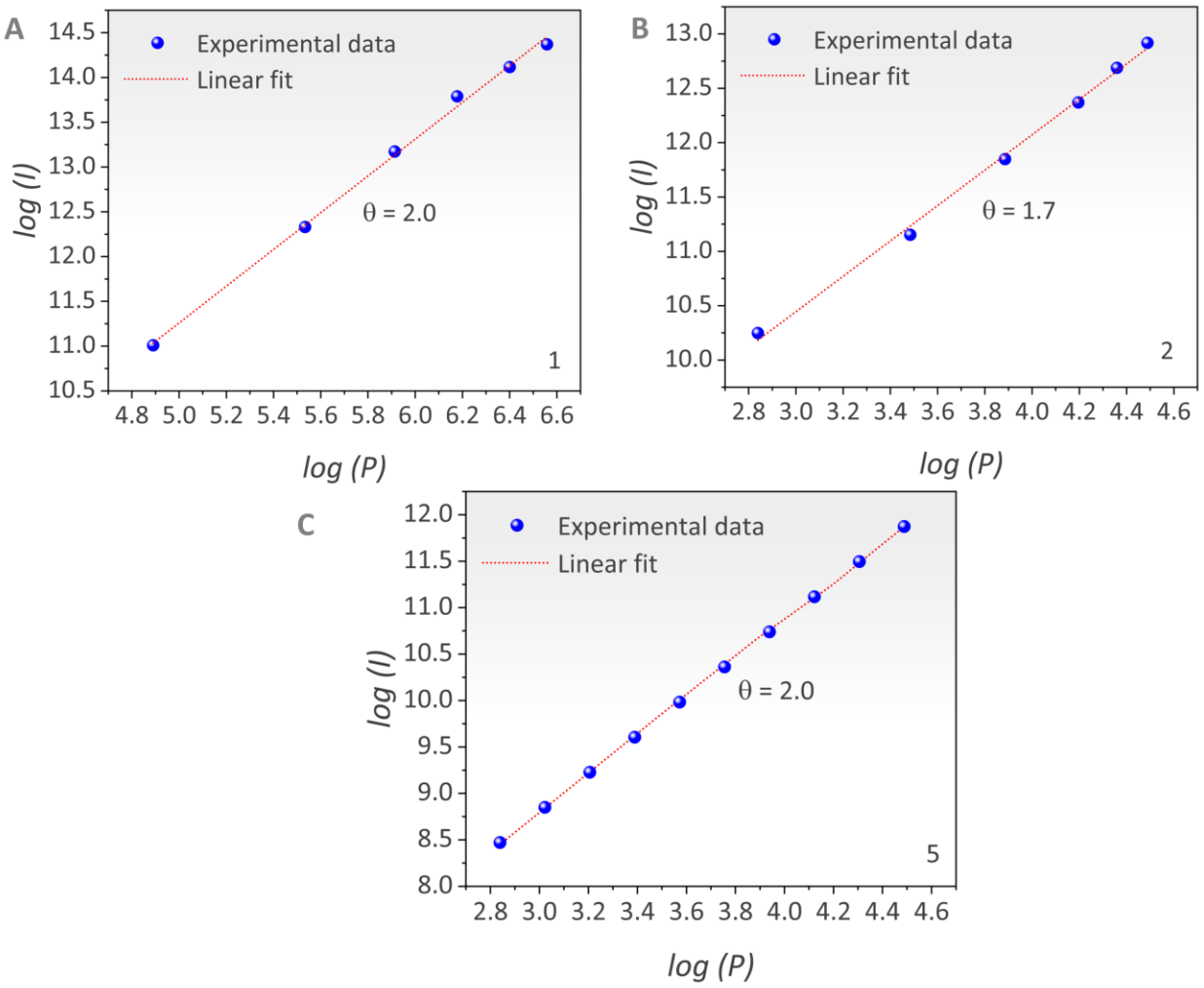

Figure S20. Intensity (*I*) dependency on the excitation power density (*P*) (in log scale) for **1**, **2** and **5**. The linear adjustment is also represented in the image ($R^2 > 0.99$).

References

[1] A. G. Bispo-Jr, L. Yeh, D. Errulat, D. A. Galico, F. A. Sigoli and M. Murugesu, *Chem. Commun.*, 2023, **59**, 8723-8726

[2] K. A. Lotsman, K. S. Rodygin, I. Skivortsova, A. M. Kutskaya, M. E. Minyaev and V. P. Ananikov, *Org. Chem. Front.*, 2023, **10**, 1022-1033

[3] G. M. Sheldrick, *Acta Cryst.,* 2015, **C71**, 3-8.

[4] G. M. Sheldrick, *Acta Cryst.,* 2008, **A64**, 112–122

[5] M. Pinsky, D. Avnir, *Inorg. Chem.*, 1998, **37**, 5575.